Effects of Substitution of Tryptophan 412 in the Substrate Activation Pathway of Yeast Pyruvate Decarboxylase†

Haijuan Li and Frank Jordan*

Departments of Chemistry and Biological Sciences and Program in Cellular and Molecular Biodynamics, Rutgers, the State University, Newark, New Jersey 07102

Received February 2, 1999; Revised Manuscript Received May 9, 1999

ABSTRACT: Oligonucleotide-directed site-specific mutagenesis was carried out on pyruvate decarboxylase (EC 4.1.1.1) from *Saccharomyces cerevisiae* at W412, located on the putative substrate activation pathway and linking E91 on the α domain with W412 on the γ domain of the enzyme. While C221 on the β domain is the residue at which substrate activation is triggered [Baburina, I., et al. (1994) *Biochemistry 33*, 5630−5635; Baburina, I., et al. (1996) *Biochemistry 35*, 10249−10255], that information, via the substrate bound at C221, is transmitted to H92 on the α domain, across the domain divide from C221 [Baburina, I., et al. (1998) *Biochemistry 37*, 1235−1244; Baburina, I., et al. (1998) *Biochemistry 37*, 1245−1255], thence to E91 on the α domain [Li, H., and Jordan, F. (1999) *Biochemistry 38*, 9992−10003], and then on to W412 on the γ domain and to the active site thiamin diphosphate located at the interface of the α and γ domains [Arjunan, D., et al. (1996) *J. Mol. Biol. 256*, 590−600]. Substitution at W412 with F and A was carried out, resulting in active enzymes with specific activities about 4- and 10-fold lower than that of the wild-type enzyme. Even though W412 interacts with E91 and H115 via a main chain hydrogen bond donor and acceptor, respectively, there is clear evidence for the importance of the indole side chain of W412 from a variety of experiments: thermostability, fluorescence quenching, and the binding constants of the thiamin diphosphate, and circular dichroism spectroscopy, in addition to conventional steady-state kinetic measurements. While the substrate activation is still prominent in the W412F variant, its level is very much reduced in the W412A variant, signaling that the size of the side chain is also important in positioning the amino acids surrounding the active center to achieve substrate activation. The fluorescence studies demonstrate that W412 is a relatively minor contributor to the well-documented fluorescence of apopyruvate decarboxylase in its native state. The information about the W412 variants provides strong additional support for the putative substrate activation pathway from C221 → H92 → E91 → W412 → G413 → thiamin diphosphate. The accumulating evidence for the central role of the β domain in stabilizing the overall structure is summarized.

In a series of papers from this laboratory, we have accumulated supporting evidence which shows that substrate activation of the thiamin diphosphate (ThDP)-dependent yeast pyruvate decarboxylase (PDC,[1] EC 4.1.1.1; for the reaction, see Scheme 1; for lead references, see refs *1*−*7*) is triggered by interaction of pyruvate (in a covalent or noncovalent fashion) with C221 on the β domain (refs *8*−*12* and the accompanying paper). Data were presented for our working hypothesis that H92 on the α domain, across the domain divide from C221, is the recipient of the information from the substrate bound at C221, with H92 thereby experiencing a modest dislocation, and this dislocation is propagated to E91, the adjacent residue, as shown in the accompanying paper. The information is transmitted to the γ domain by a hydrogen bond between the side chain carboxylic acid group of E91 and the main chain NH of W412, as well as by numerous van der Waals contacts between the side chain of E91 and a short loop in the γ domain. This short loop, comprising residues 410−415, provides not only two of three conserved hydrogen bonds to the aminopyrimidine ring of ThDP (I415 to N3′, G413 to N4′, and the third one being from E51 to the N1′ atom; *13*, *14*) but also the bulky hydrophobic side chain of I415, a residue whose role in supporting the "V" conformation and helping to create a hydrophobic environment was recently elucidated (*15*). An important consequence of the V ThDP conformation imposed by the enzyme is that the N4′ atom of the aminopyrimidine and the key C2 thiazolium atom are brought into close proximity, less than 3.2 Å from each other (*14*). According to our working hypothesis, the conserved hydrogen bond between E51 and N1′ stabilizes the imino tautomeric form of the ThDP, whose N4′ imino nitrogen is basic enough, and optimally oriented by the G413 C═O to

† Supported by NIH Grant GM-50380, NSF Training Grant BIR 94/13198 in Cellular and Molecular Biodynamics (F.J., principal investigator), the Rutgers University Busch Biomedical Fund, and Hoffmann La Roche Diagnostics Inc. (Somerville, NJ).

* To whom correspondence should be addressed. Telephone: (973) 353-5470. Fax: (973) 353-1264. E-mail: frjordan@newark.rutgers.edu.

[1] Abbreviations: ThDP, thiamin diphosphate; PDC, pyruvate decarboxylase (EC 4.1.1.1); scpdc1, wild-type pyruvate decarboxylase isolated from *Saccharomyces cerevisiae*; WT, wild-type yeast PDC enzyme overexpressed in *Escherichia coli*; W412F and W412A, variants of PDC; SDS−PAGE, sodium dodecyl sulfate−polyacrylamide gel electrophoresis; PMSF, phenylmethanesulfonyl fluoride; n_H, Hill coefficient.

10.1021/bi9902440 CCC: $18.00
Published on Web 07/15/1999

Scheme 1

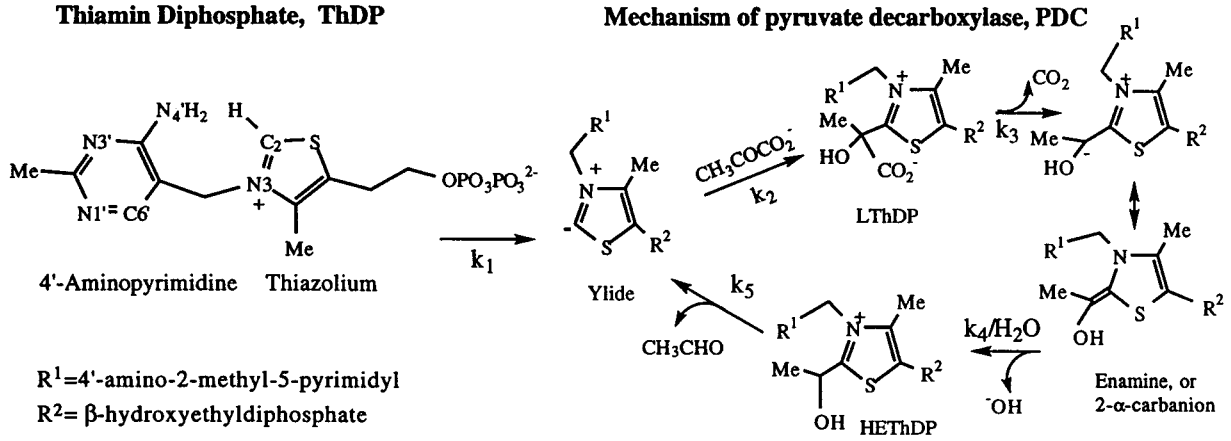

HN4′ hydrogen bond, to deprotonate the C2 atom, the first step in any ThDP-dependent reaction. The importance of this glutamic acid 51 in yeast PDC has been confirmed by substitution at this position in PDC (*7*, *16*−*18*), and also at the corresponding residue in transketolase (*19*). The X-ray structure of yeast PDC shows that the main chain C═O of W412 also forms a hydrogen bond to the imidazolyl NH atom of H115 on the α domain of a different subunit. A pair of histidines (H114 and H115 in yeast PDC and H113 and H114 in *Zymomonas mobilis* PDC) are found to be conserved among all known PDC protein sequences from yeast, bacteria, fungi, and plants (*20*). A recent study on *Z. mobilis* PDC suggested that one of the two histidines, H113, is involved in substrate binding and mediates the opening and closing of the active site by ion pairing with the carboxyl group of pyruvate (*20*). Preliminary results with yeast PDC (*7*) showed that the H114F and H115F single substitutions have no effect on the Hill coefficient, while the H114F/H115F doubly substituted PDC exhibits impairment of substrate activation. To elucidate the function of W412 at this key interdomain and intersubunit interface, and to examine its potential participation in our putative substrate activation pathway, we carried out site-directed mutagenesis studies at this position, resulting in the W412F and W412A variants. The effects of these substitutions on steady-state kinetics, substrate binding, thermostability, and conformational changes are presented.

EXPERIMENTAL PROCEDURES

Materials. The *Bam*HI restriction enzyme and the corresponding buffer were purchased from Promega. The HiLoad Q HP column was purchased from Amersham Pharmacia Biotech. Other reagents that were used were described elsewhere.

Construction of W412F and W412A Variants of PDC. Mutagenesis reactions were performed according to the PCR megaprimer method (*21*) as described in the previous paper. The oligonucleotides 5′-CTCTCAAGTCTTA**TTC**GGATCCATTGGTTTCACC-3′ [changed the tryptophan at position 412 to phenylalanine (bold) and created a *Bam*HI restriction site for mutant screening by silent mutations from GGTTCC to GGATCC (underlined)] and 5′-CTCTCAAGTCTTA-**GCG**GGATCCATTGGTTTCACC-3′ [changed the tryptophan at position 412 to alanine (bold) and created a *Bam*HI restriction site for mutant screening by silent mutations from GGTTCC to GGATCC (underlined)] were used as mutagenic primers, and oligonucleotides 5′-GTTATGCTAGTTAT-TGCTCAGCGGT-3′ and 5′-CCGCGAAATTAATACGACT-CACTATA-3′ were used as flanking primers in the first and second round of PCR, respectively. The mutation was screened by digestion with *Bam*HI. The pET22b(+):*PDC1* fragment possesses only one *Bam*HI restriction site and produces a linear fragment upon digestion with *Bam*HI. Because one additional *Bam*HI restriction site was created by site-directed mutagenesis for the W412F and W412A variants, the restriction digestion gives a 6.6 kb fragment and a 0.58 kb fragment. The desired mutations were further confirmed by DNA sequence analysis (*22*) using the primer 5′-CCACTCCGACCACATGAAGATCAGAAACGC-3′. Cultures of *Escherichia coli* strain BL21(DE3) were transformed with the mutated plasmids, as described previously (*22*).

DNA sequencing, enzyme assay, steady-state kinetic assays, apoenzyme preparation, circular dichroism, and fluorescence and thermostability measurements were carried out as described in the accompanying paper.

Overexpression and purification of PDC were carried out as described in the accompanying paper except for the use of a HiLoad Q HP column for ion exchange chromatography.

Steady-State Kinetic Studies. The effect of pH on the steady-state kinetic properties of PDC was determined as described elsewhere (refs *11* and *15* and the accompanying paper). For the buffer, we used a mixture of 50 mM MES, 100 mM Tris, and 50 mM acetic acid, adjusted to the desired pH with NaOH or HCl. This three-component buffer maintains a constant ionic strength over a wide range of pH values (*23*).

RESULTS

Site-Directed Mutagenesis and Expression and Purification of the W412A and W412F Variants of PDC

The W412A and W412F variants of PDC were constructed using the megaprimer PCR method. A new *Bam*HI restriction site was introduced via a silent mutation, and this was used to screen for the desired mutations. Mutations were further confirmed by DNA sequencing (*22*).

The expression of the W412A and W412F variants in *E. coli* resulted in active enzymes. All enzymes were purified on a HiLoad Q column. The fractions of W412F variant with the highest purity eluted from the column had a specific

Table 1: Steady-State Kinetic Parameters of WT and Its W412 Variants in 0.1 M MES Buffer at pH 6.0 and 25 °C

	specific activity (units/mg)	$S_{0.5}$ (mM)	k_{cat} (s^{-1})	$k_{cat}/S_{0.5}$ (mM^{-1} s^{-1})	n_H
WT	60.0 ± 5.0	1.09 ± 0.17	73.1 ± 1.4	67.1 ± 0.2	2.18 ± 0.05
W412F	15.8 ± 1.3	0.82 ± 0.03	17.8 ± 0.2	19.2 ± 0.5	1.93 ± 0.06
W412A	6.40 ± 0.53	4.19 ± 0.43	6.55 ± 0.65	1.56 ± 0.01	1.30 ± 0.13

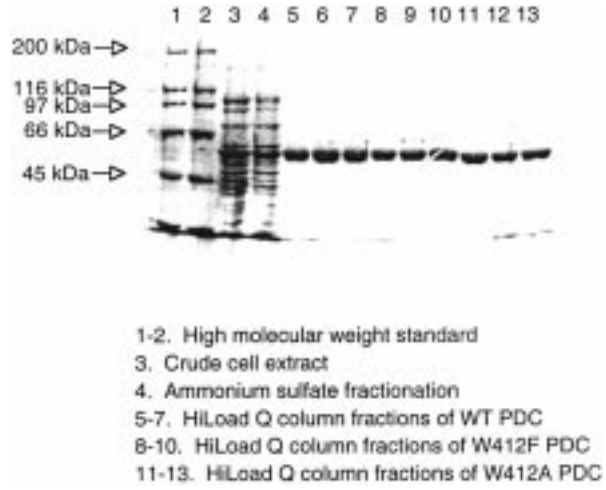

FIGURE 1: SDS−PAGE analysis for the purification of WT and W412A and W412F PDC. High-molecular mass markers with molecular masses are denoted on the left: myosin (200 kDa), β-galactosidase (116.3 kDa), phosphorylase *b* (97.4 kDa), serum albumin (66.2 kDa), and ovalbumin (45 kDa).

activity of 16−18 units/mg (Table 1). When fully activated with cofactors, the W412A variant had a final specific activity of 6.4 units/mg (Table 1). Both enzymes were purified to apparent homogeneity as judged by SDS−PAGE (Figure 1).

Characterization of W412A and W412F Variants of PDC

Steady-State Kinetics. The Michaelis−Menten plots are presented in Figure 2, while the steady-state kinetic parameters of the W412 PDC variants are compared with those for WT in Table 1. The specific activity of the W412F variant is reduced by a factor of 4, and of the W412A by a factor of 10, in the same relative order as the reductions in turnover number (k_{cat}) and catalytic efficiency ($k_{cat}/S_{0.5}$). At pH 6.0, the W412A substitution led to a reduction in the Hill coefficient from 2.0 to 1.3 and a 4-fold increase in $S_{0.5}$. In contrast, the Hill coefficient and $S_{0.5}$ were not significantly altered by the W412F substitution, indicating that substitution of W412 with F had not significantly disturbed the active site and substrate activation.

pH Dependence of Steady-State Kinetic Parameters. The pH dependence of steady-state kinetic parameters (please see the accompanying paper for definitions of *V*, *V*/*A*, *V*/*B*, k_{cat}, $S_{0.5}$, $k_{cat}/S_{0.5}$, and n_H) was determined for WT (Figure S1 of the Supporting Information) and the W412F (Figure S2 of the Supporting Information) and W412A variants (Figure S3 of the Supporting Information). A summary of the pH dependence of steady-state kinetic parameters is presented in Tables 2−4. The values of pK_{app} were determined from the kinetic constant−pH plots, and are presented in Table 5. In this study, a three-component buffer (50 mM MES, 100 mM Tris, and 50 mM acetic acid) was used to keep the ionic strength constant over a wide range of pH values instead of using different buffers for the different pH ranges used in the accompanying paper. The three-component buffer caused a decrease in n_H by 0.2 compared to the buffers used elsewhere, but had only a small or no effect on other steady-state kinetic properties. As seen for the E91 variants in the accompanying paper, the most striking differences are observed in the Hill coefficients (Figure 3). For WT and the W412F variant, n_H is pH-dependent with a maximum value of 1.8−1.9 at the pH optimum of 6.0; for the W412A variant, n_H is pH-independent with a value of 1.2−1.3. The k_{cat}−pH profiles have similar shapes for WT and W412 variants, but the values of pK_{app} become more acidic in the variants than in WT. However, there is a notable difference in $k_{cat}/S_{0.5}$−pH plots. The pK_{app} in the acidic region is absent in the W412 variants, and the single pK_{app} that can be observed has experienced a shift to the acidic region by 0.3−0.5 pH unit, suggesting that the entire bell-shaped curve has experienced an acid shift.

Thermostability of WT and W412 Variant Enzymes. The structural stability of WT and W412 variants was evaluated by measuring the temperature dependence of the activity loss (Figure 4). The substitutions reduced the thermostability. The T_m is 59.5 °C for WT and 51.5 °C for the W412F and 40.0 °C for the W412A variant. The thermostability diminished in the same order as the specific activity (WT > W412F > W412A).

ThDP Binding According to the Quenching of Apoenzyme Fluorescence. The WT exhibited an emission maximum of intrinsic fluorescence at 338 nm when excited at 300 nm (*22*). Substitution of W412 with F resulted in a blue shift of the wavelength of maximum emission to 335 nm (*22*), indicating that W412 is internal and is located in a hydrophobic environment on the enzyme. The quenching of fluorescence was concentration-dependent and saturable and followed a hyperbolic curve just as seen with WT (*22*). However, the W412A variant was not saturated by ThDP in the experimentally accessible concentration range, suggesting a relatively low affinity for the ThDP, as determined from the quenching of the intrinsic apoenzyme fluorescence upon cofactor binding (Figures 5) (*24*, *25*). The W412F variant exhibited behavior very similar to that of WT in its fluorescence quenching parameters, while the W412A substitution had a dramatic effect on ThDP binding (Table 6). The dissociation constant for ThDP in the W412A variant was 666 μM, estimated from the curve fitting at higher ThDP concentrations, substantially higher than that for WT. In contrast, the affinity of the W412F variant for ThDP was indistinguishable from that of WT (Table 6). This result is reinforced by the finding that, for the W412A variant only, the cofactors could be separated by ion-exchange or gel filtration chromatography at pH 6.0 during the purification. Moreover, the great reduction in the affinity of the W412A variant for ThDP may result in the underestimation of its specific activity with the standard activity assay.

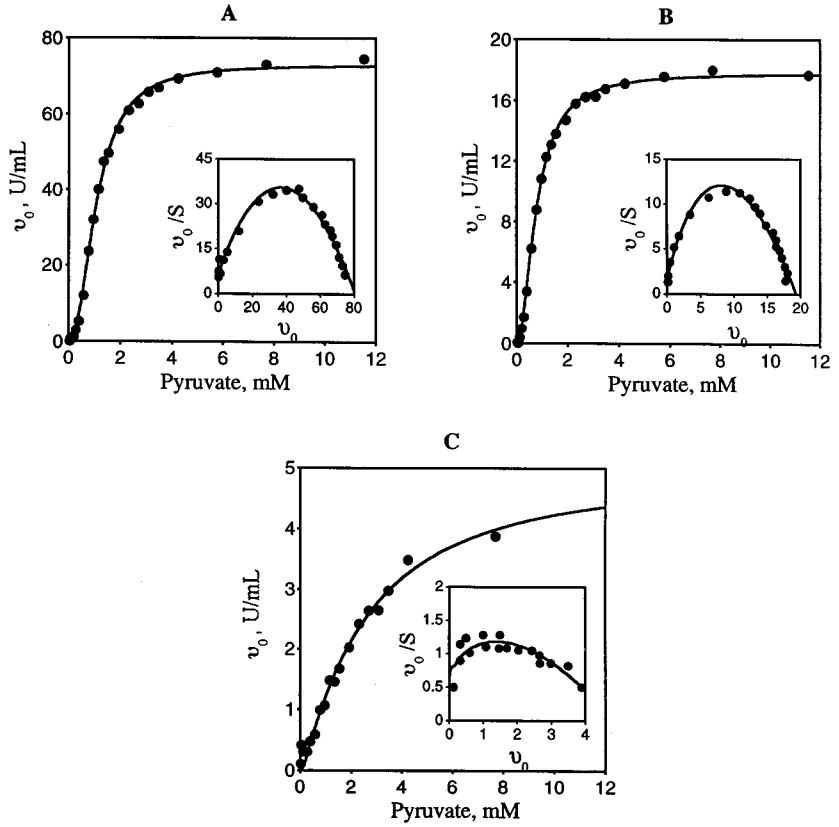

FIGURE 2: v_0-S plots for WT (A), W412F PDC (B), and W412A PDC (C) in 100 mM MES at pH 6.0 and 25 °C. The insets are Eadie−Scatchard plots.

Table 2: Steady-State Kinetic Data for WT

pH	n_H	k_{cat} (s^{-1})	$S_{0.5}$ (mM)	$k_{cat}/S_{0.5}$ (mM^{-1} s^{-1})	V (mM min^{-1})	V/A (mM^{-1} min^{-1})	V/B (min^{-1})
4.50	1.24 ± 0.09			4.2 ± 0.5			504 ± 10
4.70	1.29 ± 0.12			8.7 ± 1.0			443 ± 7
5.00	1.31 ± 0.09	25.6 ± 1.1	1.29 ± 0.13	19.9 ± 1.2	121 ± 4	100 ± 12	482 ± 50
5.30	1.54 ± 0.05	46.3 ± 0.7	1.21 ± 0.05	38.1 ± 1.0	221 ± 3	246 ± 16	434 ± 45
5.50	1.63 ± 0.05	54.0 ± 0.7	1.23 ± 0.05	43.9 ± 1.2	258 ± 3	326 ± 23	385 ± 31
5.70	1.68 ± 0.05	59.6 ± 0.6	1.24 ± 0.04	48.1 ± 1.1	284 ± 3	400 ± 29	369 ± 24
6.00	1.76 ± 0.05	70.2 ± 0.9	1.34 ± 0.05	52.5 ± 1.3	327 ± 4	448 ± 38	314 ± 20
6.30	1.71 ± 0.05	67.9 ± 1.0	1.55 ± 0.07	43.9 ± 1.3	316 ± 5	355 ± 32	253 ± 15
6.50	1.64 ± 0.06	67.1 ± 1.1	1.70 ± 0.08	39.5 ± 1.2	312 ± 5	339 ± 40	194 ± 16
6.70	1.45 ± 0.08	59.1 ± 2.1	1.86 ± 0.15	31.8 ± 1.4	292 ± 5	143 ± 25	58 ± 11
7.00	1.32 ± 0.06	44.3 ± 1.0	2.42 ± 0.15	18.3 ± 0.7	221 ± 9	90 ± 11	22 ± 3
7.30	1.29 ± 0.06		3.10 ± 0.23	19.1 ± 1.4			
7.50			4.08 ± 0.53	10.9 ± 1.4			

Table 3: Steady-State Kinetic Data for the W412A Variant of PDC

pH	n_H	k_{cat} (s^{-1})	$S_{0.5}$ (mM)	$k_{cat}/S_{0.5}$ (mM^{-1} s^{-1})	V (mM min^{-1})	V/B (min^{-1})
5.00	1.16 ± 0.14	1.18 ± 0.06	0.58 ± 0.12	2.04 ± 0.16	8.2 ± 0.3	13.6 ± 2.4
5.30	1.07 ± 0.11	3.47 ± 0.37	1.11 ± 0.29	3.13 ± 0.48	21.0 ± 3.1	22.9 ± 1.2
5.50	1.12 ± 0.16	3.77 ± 0.35	1.81 ± 0.32	2.08 ± 0.18	27.4 ± 1.6	12.0 ± 2.4
5.70	1.23 ± 0.13	6.01 ± 0.60	2.55 ± 0.43	2.36 ± 0.16	44.3 ± 4.3	15.8 ± 2.8
6.00	1.27 ± 0.21	6.37 ± 0.17	4.19 ± 1.93	1.52 ± 0.65	54.6 ± 0.5	15.7 ± 3.4
6.30	1.29 ± 0.19	3.54 ± 0.25	7.77 ± 1.25	0.45 ± 0.04	25.6 ± 1.7	7.6 ± 2.9
6.50	1.02 ± 0.14	2.97 ± 0.12	19.0 ± 1.9	0.16 ± 0.01	12.4 ± 1.0	5.4 ± 1.7
6.70	1.00 ± 0.22	2.20 ± 0.54	34.6 ± 4.1	0.06 ± 0.01	15.2 ± 0.1	1.7 ± 1.8

The double-reciprocal plot of $1/[(F_0 - F)/F_0 \times 100]$ versus 1/[ThDP] and the modified Stern−Volmer plot for the W412F variant are nearly linear, just as seen for the WT, suggesting only one class of ThDP binding sites (data not shown). This was further confirmed by the value of 0.4 for the accessible fraction f_a (Table 6). In contrast, those for the W412A variant were biphasic with two linear regions. The substitution may induce a conformational change on the enzyme which results in two different classes of ThDP binding sites with different K_d values: a high-affinity type and a low-affinity type.

The Stern−Volmer plot if the W412A variant exhibited upward curvature, indicating the occurrence of both collisional and static quenching processes and the presence of more than one fluorophore in the enzyme. On the other hand, the W412F variant exhibited a downward-curving Stern−

Table 4: Steady-State Kinetic Data for the W412F Variant of PDC

pH	n_H	k_{cat} (s^{-1})	$S_{0.5}$ (mM)	$k_{cat}/S_{0.5}$ (mM^{-1} s^{-1})	V (mM min^{-1})	V/A (mM^{-1} min^{-1})	V/B (min^{-1})
4.50	1.15 ± 0.24	1.3 ± 0.1			6.4 ± 0.4		
4.70	1.24 ± 0.20	2.1 ± 0.1			10.5 ± 0.6		
5.00	1.54 ± 0.04	9.8 ± 0.1	0.30 ± 0.01	39.1 ± 1.3	49.6 ± 0.4	652 ± 32	991 ± 132
5.30	1.72 ± 0.06	11.8 ± 0.1	0.37 ± 0.02	37.3 ± 0.1	60.5 ± 0.6	658 ± 60	
5.50	1.79 ± 0.05	12.7 ± 0.1	0.40 ± 0.01	36.4 ± 0.7	64.5 ± 0.5	461 ± 28	1024 ± 219
5.70	1.85 ± 0.06	13.2 ± 0.1	0.52 ± 0.02	29.1 ± 0.1	77.4 ± 1.1	352 ± 28	645 ± 93
6.00	1.94 ± 0.09	15.8 ± 0.4	0.82 ± 0.08	19.2 ± 0.1	80.3 ± 2.0	143 ± 17	472 ± 66
6.30	1.82 ± 0.05	13.6 ± 0.1	1.14 ± 0.04	13.7 ± 0.3	70.5 ± 1.1	67.8 ± 9.2	227 ± 32
6.50	1.70 ± 0.06	13.4 ± 0.2	1.58 ± 0.08	9.8 ± 0.3	70.9 ± 13.7	44.3 ± 4.0	101 ± 17
6.70	1.64 ± 0.03	13.0 ± 0.1	1.99 ± 0.04	7.5 ± 0.9	69.3 ± 0.9	30.9 ± 1.7	64.2 ± 5.5
7.00	1.55 ± 0.05	10.4 ± 0.2	3.04 ± 0.09	4.1 ± 0.1	58.2 ± 1.9	14.4 ± 1.7	25.4 ± 3.1
7.30	1.48 ± 0.08	8.8 ± 0.5	4.37 ± 0.25	2.5 ± 0.1	52.5 ± 3.8		
7.50	1.24 ± 0.30	8.7 ± 0.4	8.21 ± 0.29	1.3 ± 0.1	57.0 ± 3.1		

Table 5: Apparent pK_a Data for WT and Its W412A and W412F Variants Estimated from pH-Dependent Kinetic Parameters[a]

kinetic constant	WT		W412A		W412F	
	pK_{a1}	pK_{a2}	pK_{a1}	pK_{a2}	pK_{a1}	pK_a
k_{cat}	5.4	7.0	closer than 1 unit ca. 5.5 and 6.3		5.20	7.2
$k_{cat}/S_{0.5}$	5.5	6.5	ND[b]	6.0	ND[b]	6.0
V/A	5.5	6.5	ND[b]	6.0	ND[b]	5.9
V/B	ND[b]	6.0−6.5	ND[b]	6.0	ND[b]	5.5

[a] The results were obtained from both semilog (kinetic constant−pH) and log−log [log(kinetic constant)−pH] plots; pK_{a1} and pK_{a2} refer to the apparent values determined on the acid and alkaline side of the curves, respectively. The estimated error is ±0.3 unit on fitting the data from Tables 2−4 and shown in Figures S1−S3 in the Supporting Information to a Dixon−Webb equation by a nonlinear least-squares method. [b] No values could be estimated from the data due to the absence of an apparent pH dependence in the pH range that was examined, or the pH dependence not being readily interpretable.

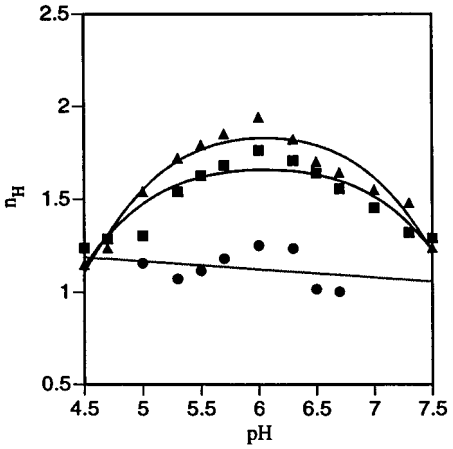

FIGURE 3: pH dependence of the Hill coefficient for WT (■) and its W412F (▲) and W412A (●) variants.

Volmer plot, similar to that of WT, suggesting that only collisional quenching was observed.

Changes in Tertiary Structure According to Circular Dichroism Studies. The CD spectra of WT and W412 variants are shown in Figure 6. As discussed in the accompanying paper, the binding of ThDP to the WT apoenzyme induced a characteristic two-signal dichroic peak with a positive maximum at 263 nm, a negative maximum at 283 nm, and a weak negative diffuse band over the 300−360 nm region. Although the CD spectra of the three apoenzymes were very similar (Figure 6), the CD spectra exhibited a significant difference upon ThDP binding. The

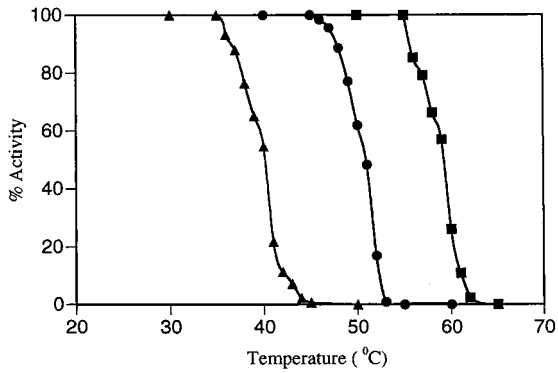

FIGURE 4: Thermostability of WT (■) and its W412F (●) and W412A variants (▲).

Table 6: Parameters for Quenching the Intrinsic Fluorescence of Apo-WT and Its W412 Variants upon Addition of Cofactors

	apparent K_d (μM)	maximal quenching (%)	f_a
WT	20.6 ± 5.5[a,b]	29.1 ± 6.9[a,b]	0.29 ± 0.07[a,b]
W412A	58.6 ± 23.9[a]	26.1 ± 14.6[a]	0.11 ± 0.06[a]
	666 ± 105[b]	100 ± 18.0[b]	1.0 ± 0.2[b]
W412F	21.2 ± 4.2[a,b]	38.3 ± 6.9[a,b]	0.42 ± 0.07[a,b]

[a] The values obtained with 1−12 μM ThDP. [b] The values obtained with 12−500 μM ThDP.

W412F variant had a distinctly broadened positive peak with the maximum at 263 nm and a weakening negative peak with the maximum at 283 nm, while the negative diffuse peak in the 300−360 nm range was absent. In contrast, the W412A variant did not exhibit any positive peaks, but only a weakened and broadened negative peak at 258 nm and a larger negative diffuse peak between 280 and 360 nm.

The temperature dependence of the near-UV CD spectra provides a means of evaluating side chain packing interactions. Native proteins with well-packed side chains usually undergo a cooperative thermal transition upon increases in temperature, whereas non-well-packed or partially folded variant enzymes do not exhibit such cooperativity. As shown in Figure 7, WT unfolds cooperatively at 43 °C according to the CD experiment unlike the W412F variant which did not show a cooperative thermal unfolding behavior, suggesting disrupted side chain packing.

DISCUSSION

This study reports the first evidence in support of our working hypothesis for involvement of W412 in the substrate

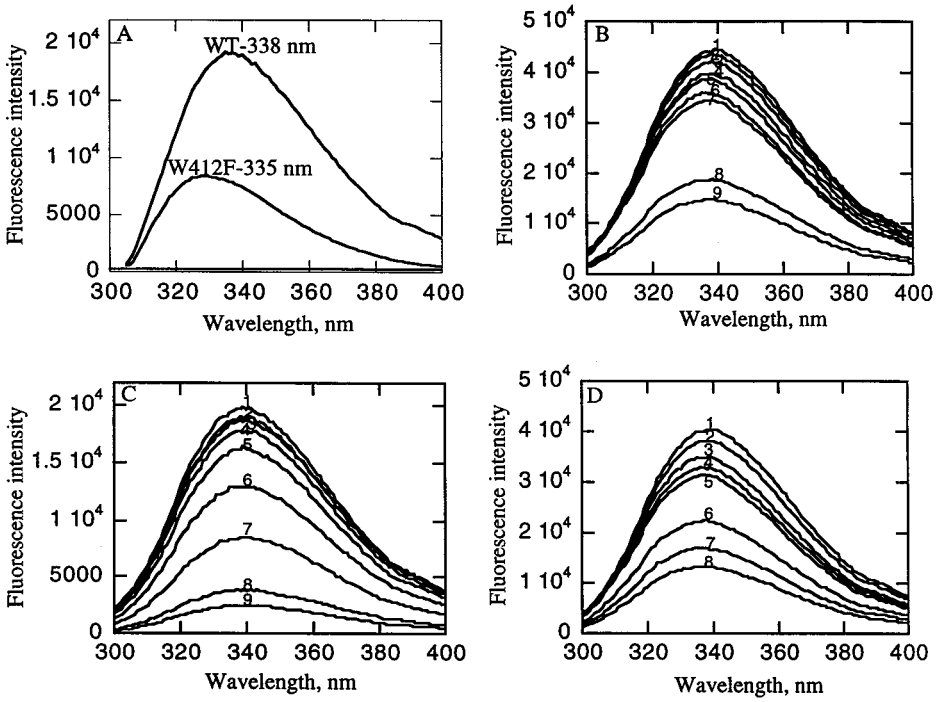

FIGURE 5: (A) Intrinsic fluorescence emission spectra of WT and its W412F variant. Excitation was at 290 nm in 10 mM MES (pH 6.0) containing 1 mM ThDP and 10 mM Mg(II). The fluorescence emission maximum wavelength is 338 nm for WT and 335 nm for W412F. (B) Effect of ThDP on the fluorescence emission spectrum of WT. The enzyme (0.1 mg/mL) was preincubated with 10 mM Mg(II) in 100 mM MES (pH 6.0), and then the following concentrations of ThDP were added: (1) 0, (2) 1.55, (3) 3.10, (4) 6.20, (5) 12.38, (6) 24.74, (7) 30.90, (8) 162.93, and (9) 228.81 μM. The excitation wavelength was 290 nm. (C) Effect of ThDP on the fluorescence emission spectrum of W412A PDC. The enzyme (0.1 mg/mL) was preincubated with 10 mM Mg(II) in 100 mM MES (pH 6.0), and then the following concentrations of ThDP were added: (1) 0, (2) 3.41, (3) 6.81, (4) 13.61, (5) 40.79, (6) 88.34, (7) 190.09, (8) 391.63, and (9) 494.11 μM. The excitation wavelength was 290 nm. (D) Effect of ThDP on the fluorescence emission spectrum of W412F PDC. The enzyme (0.1 mg/mL) was preincubated with 10 mM Mg(II) in 100 mM MES (pH 6.0), and then the following concentrations of ThDP were added: (1) 0, (2) 3.10, (3) 12.38, (4) 18.56, (5) 30.90, (6) 96.95, (7) 162.93, and (8) 228.81 μM. The excitation wavelength was 290 nm.

activation pathway in yeast PDC. To evaluate the role of this residue, it was replaced using site-directed mutagenesis by phenylalanine, as a conservative replacement, and alanine, as a nonconservative replacement.

The variant and WT enzymes could be purified by the same method, but the W412A variant could only be purified as an apoenzyme. Like WT, the purified W412F variant retains its activity and positive cooperativity unchanged for several months at 4 °C. However, the W412A variant lost most of its activity and cooperativity within 1 week. These results suggest the need for a bulky aromatic side chain at position 412 to help to stabilize the conformation at the active site, as well as to maintain the positive cooperativity. The modest reduction in kinetic parameters demonstrates that the substitutions lead to enzymes with their active centers still intact.

Kinetic Consequences of Substitutions at W412

Consequences for the Hill Coefficient. The W412A substitution resulted in a significant reduction in the Hill coefficient, clearly indicating the participation of W412 in the substrate activation pathway. A comparison of the Hill coefficient of W412F with that of WT suggests that the aromatic side chain at position 412 is very important and the substitution can functionally compensate for the loss of the aromatic chain of tryptophan. This suggestion is also supported by the pH dependence of the Hill coefficient; for W412F, it is pH-dependent like that for WT, while it is pH-independent for the W412A variant (Figure 3).

Consequences for V_{max} (k_{cat}). The shapes of the k_{cat}−pH plots for the W412 variants are similar to that for WT, but the two pK_{app} values are closer to each other for the W412A variant than for WT and the W412F variant (Figures S1−S3 of the Supporting Information and Table 5), suggesting some perturbation in the hydrogen bonding network surrounding the active site.

Consequences for $S_{0.5}$. As can be seen in Tables 2−4, the $S_{0.5}$ is reduced with decreasing pH, as found for WT and all other variants on the putative substrate activation pathway. Interestingly, $S_{0.5}$ is even more favorable for the W412F variant than for WT, while exhibiting a similar pH dependence.

The pH-dependent curve is shifted toward the acid side by about 1 pH unit for the W412A variant, indicating that it is more difficult to bind the substrate to this variant at higher pH than to the others. Given that the Hill coefficient is not significantly greater than unity, in this case $S_{0.5}$ is similar to K_m; hence, it applies to the active center, rather than to the regulatory site.

Consequences for $V/S_{0.5}$ (V/A). The W412 substitutions created a dramatic effect on the $k_{cat}/S_{0.5}$−pH (or V/A−pH) profile, suggesting that the ionizable groups of the enzyme involved in binding the first substrate (at the regulatory site C221) are being perturbed by the substitutions. Unlike that for WT, the $k_{cat}/S_{0.5}$ values for the variants did not decrease as the pH was lowered. The acidity of the group(s) responsible for the acid limb pK_{app} in the $k_{cat}/S_{0.5}$ profile in WT has been enchanced so that this group(s) is fully

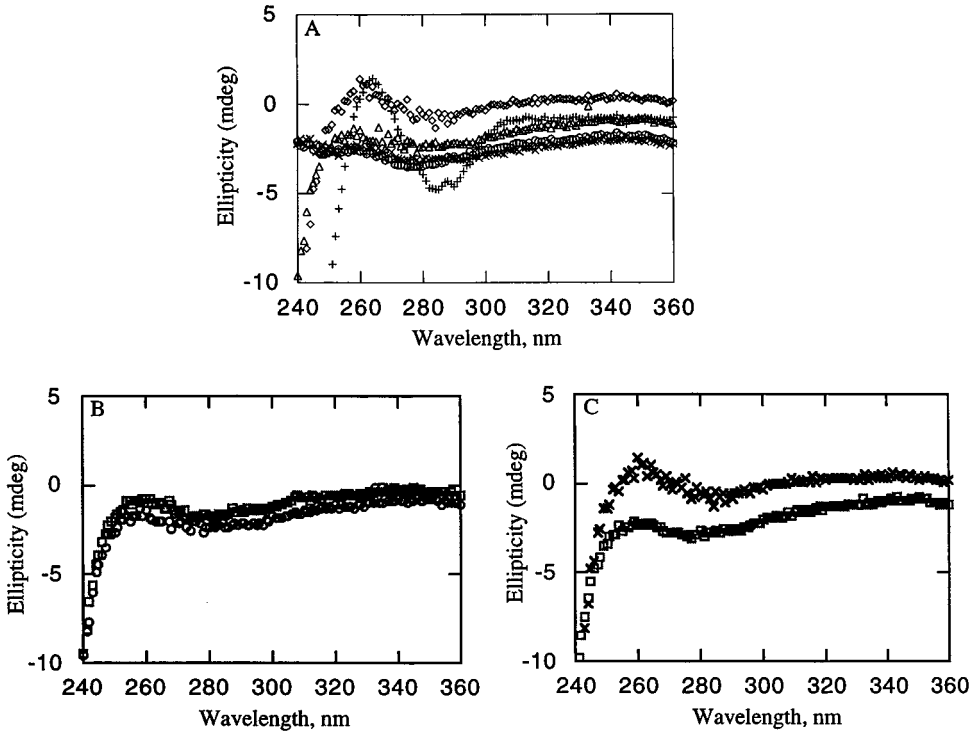

FIGURE 6: Near-UV CD spectra of WT and its W412A and W412F variants. The apoenzyme (2 mg/mL) was preincubated with 10 mM Mg(II) in 50 mM potassium phosphate at pH 6.0 and 25 °C. Then the ThDP was added, and the spectra were recorded over the 240−360 nm range, with a path length of 0.1 cm. (A) Summary showing WT (+), W412F (△), W412A (◇), 1 mM ThDP (○), and 50 mM potassium phosphate (pH 6.0) (×). (B) Near-UV CD spectra of W412A PDC. The apoenzyme (2 mg/mL) was preincubated with 10 mM Mg(II) in 50 mM potassium phosphate at pH 6.0 and 25 °C (×). Then the 1 mM ThDP was added (△). (C) Near-UV CD spectra of W412F PDC. The apoenzyme (2 mg/mL) was preincubated with 10 mM Mg(II) in 50 mM potassium phosphate at pH 6.0 and 25 °C (□). Then the ThDP was added, and the spectra were recorded over the 240−360 nm range, with a path length of 0.1 cm (×).

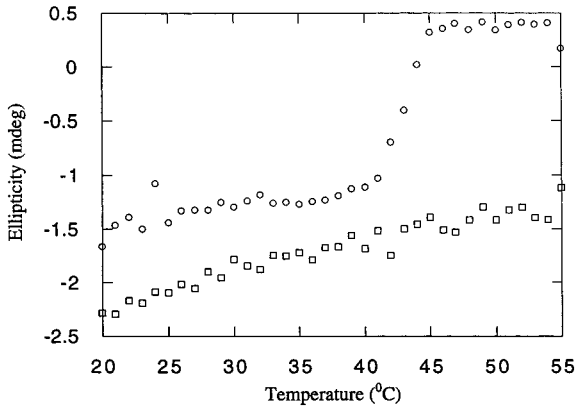

FIGURE 7: Thermally induced unfolding of WT and W412F PDC. Experiments were carried out in 1 cm path length cuvettes using 0.5 mg/mL enzyme in 50 mM potassium phosphate (pH 6.10) containing 2.5 mM $MgSO_4$ and 0.5 mM ThDP. Experimental conditions for data collection were as follows: temperature range, 20−55 °C; wavelength, 283 nm; temperature step, 1 °C; and equilibrium time, 1 min. WT (○) and W412F (□).

dissociated at pH ∼5.0. As discussed in the accompanying paper, the $k_{cat}/S_{0.5}$−pH plot reflects the energetics of transition states starting with the addition of the first pyruvate to PDC at the regulatory site, and terminating with the decarboxylation step. The results provide strong confirmation for participation of W412 in signal transmission to the active site.

Consequences for k_{cat}/B. This term corresponds to the rate-limiting step at intermediate substrate concentrations, starting with the binding of the second substrate at the catalytic center to the (already) substrate-activated enzyme. There is a progressive acid shift in these plots in going from WT to W412F to W412A, i.e., the single pK_a implied by the pH dependence. This pK_a must pertain to a group participating in the reversible addition of pyruvate to ThDP or decarboxylation. Since the same order of magnitude shift is observed in the alkaline limb of both V/A ($k_{cat}/S_{0.5}$) and V/B plots, where data can be fitted, we tentatively suggest that the same rate-limiting step is being monitored, probably the reversible addition of pyruvate to ThDP on pyruvate-activated PDC.

From the pH-dependent kinetic behavior, one can conclude that the W412 substitutions are indeed sensed at both the catalytic and regulatory sites.

Structural Consequences of Substitutions at W412

The binding of ThDP according to quenching of intrinsic fluorescence provided further proof that in the W412F variant the environment of the active site was not significantly changed. However, the W412A variant resulted in a great reduction in the affinity of the apoenzyme for ThDP (Table 6). This could be interpreted as a change in the tertiary structure, consistent with the changes in the CD spectra (see below).

The CD spectra of the W412 variants are considerably different from that of the WT. Combined with the results from steady-state kinetics, a comparison of the CD spectra with that of WT revealed the following. The interactions associated with the positive peak at 263 nm, present in all E91 and W412 variants at much attenuated strength, are characteristic of WT especially. Again, as was concluded

for the E91 variants, the absence of a strong positive peak at 263 nm and a negative one at 283 nm (much weaker in the W412F and absent in the W412A variant) has no direct correlation with enzymatic activity or activation.

The importance of the bulky aromatic side chain at position 412 has also been revealed by the temperature dependence of the CD signal (Figure 7). The absence of a cooperative thermal transition in the variant indicates looser side chain packing caused by the substitution. Both the W412A and W412F variants exhibited reduced thermostability, also supporting this suggestion. A comparison of the thermostability of the two variants underlines the importance of an aromatic side chain at position 412. The destabilization of the enzyme by substitution of W412 with an amino acid without an aromatic side chain, such as alanine, can be ascribed to two non-mutually exclusive factors. First, replacement of W412 with A may increase the flexibility of the backbone around this residue and thus directly abolish or weaken its concurrent hydrogen bonds with E91 and H115. Second, the W412A substitution may have perturbed the hydrogen bonding network in the active site and altered the orientation of ThDP binding indirectly. The increased flexibility of the backbone at position 412 certainly has an impact on the adjacent position of G413, as well as on the loop comprising residues 410−415. As mentioned above, G413 and I415 provide two of three conserved hydrogen bonds to the aminopyrimidine ring of ThDP (*6*). It was proposed that the correct positioning of the hydrogen bonds may indeed be responsible for the substrate activation event (*7*).

Summary of Findings for the Putative Substrate Activation Pathway

The substrate activation phenomenon has been identified for all known PDCs from different species so far (*27*, *28*), except for PDC from the bacterium *Z. mobilis* (*24*). In yeast PDC, C221 was identified as regulatory site for substrate or analogue binding (*8*−*12*). On the basis of the X-ray crystal structure of yeast PDC (*13*), modeling studies by Lobell and Crout (*29*) suggested that docking of pyruvate at C221, possibly through the formation of a covalent hemithioketal, could be facilitated by two hydrogen bonds between pyruvate and the NH and OH of S311 in a very favorable, energy-minimized docking position. Alvarez et al. (*30*) carried out extensive kinetic isotope effect studies with yeast PDC. They interpreted the results with a model according to which the addition and elimination of pyruvate at C221 are coupled to opening and closing of the active site. The substrate activation phenomenon is also observed for PDC from plants (*31*). However, there is no cysteine conserved between yeast PDC and plant PDC, and the amino acid in plant PDC corresponding to position C221 in yeast is a lysine (*32*), as it is for the PDC from *Z. mobilis*. Chemical modification of plant PDC with cysteine-specific reagents suggested that SH groups may be involved in the substrate activation process, but they may not play the same crucial role as in yeast PDC (*31*).

The crystal structures of yeast PDC in the presence of the activator pyruvamide (*33*) and ketomalonate (*34*) have been determined. In the presence of pyruvamide, the tetramer has more compact structure and the active site appears to be more accessible when pyruvamide is absent. In contrast, the crystal structure in the presence of ketomalonate is the open form, consistent with the modeling study which shows that the open form of the tetramer is the active form of the enzyme (*29*). Surprisingly, in neither study could the binding of the activators at C221 be observed because of weak electron density. On the other hand, there is direct protein chemical evidence for the high reactivity of C221 toward electrophiles (*12*). A more detailed analysis and comparison is required to establish the significance of the different tetramer assemblies identified for the substrate activation mechanism. So far, different crystal structures of yeast PDC have revealed that large conformational changes in the enzyme, involving both loop closure at the active site and tetramer reassembly, are triggered by the activator molecules. Recently, the crystal structure of PDC from *Z. mobilis* was reported (*35*). The interface region between the two dimers is much larger in *Z. mobilis* PDC than in yeast PDC. It was suggested that the tight packing of the dimers in the tetramer prevents the occurrence of the large conformational changes seen in the yeast PDC during the substrate activation event, and it was claimed that this locks the enzyme in an activated conformation. Unfortunately, the structure was determined with a decomposed form of ThDP, lacking the key C2 atom; hence, conclusions about the active center should be viewed with caution. In any event, using *Z. mobilis* PDC as a structural model for the substrate-activated form of yeast PDC is dangerous given the extent of overall homology between the two enzymes, notwithstanding a higher degree of apparent homology at the active center.

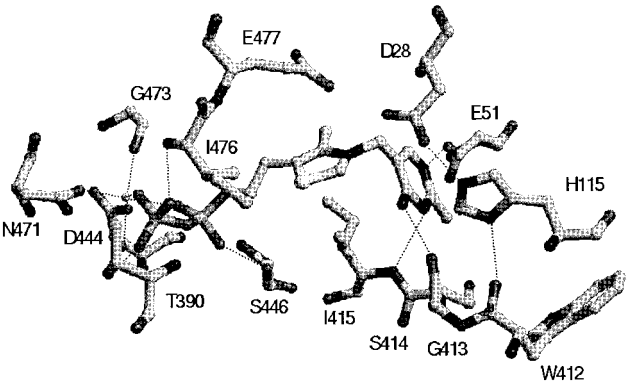

FIGURE 8: Location of W412 with respect to ThDP on yeast PDC. Residues H115 and lower are on a subunit different from that for residues 410−415.

The crystal structure of yeast PDC revealed that C221 on the β domain is roughly 20 Å away from the C2 atom of ThDP at the active site located between the α and γ domains; hence, the signal from pyruvate at C221 must somehow be propagated across this distance. On the basis of the crystal structure of the enzyme, a putative substrate activation pathway was postulated by molecular modeling (*34*). As seen in Figure 8, and Figure 7 in the accompanying paper, from the structure one could imagine how binding substrate at the regulatory site C221 on the β domain could lead to perturbations in the neighboring α domain, eventually propagating a signal to critical elements of the active site via the loop of residues 410−415 in the γ domain. It had been demonstrated that the perturbation caused by covalently binding an inhibitor to C221, or reversible binding of regulatory molecules at this site, could indeed be propagated

across these domains and result in distortions at the active site (*11*, *12*). The series of site-directed mutagenesis experiments presented in ref *11*, as well as in the accompanying paper and this paper, involving H92, E91, and W412, provide strong evidence supporting this working putative substrate activation pathway.

It is also important to emphasize that PDC that is devoid of the cooperativity signaled by substrate activation (due to substitutions of amino acids in our putative substrate activation pathway) is still a reasonably active enzyme, just as is PDC from *Z. mobilis*. While the activity of yeast PDC is regulated by binding of the substrate to the regulatory site C221, this substrate activation is not absolutely required for the PDC to maintain its activity.

The results add to the accumulating evidence for the importance of the β domain in PDC activity and stabilization. While not involved in cofactor binding, several lines of evidence now indicate that the β domain serves rather important functions in addition to the regulatory one identified in this series of papers. For example, the D291N substitution, and the deletion of S296 and F297, all three in a flexible loop not resolved in the yeast PDC structures in the absence of activators, lead to a 30000-fold decrease in specific activity and much reduced stability (*22*, *36*), as do some of the substitutions at R224 (*22*), all in the β domain. A simple explanation is that the β domain helps to hold the α and γ domains in the appropriate conformation for ThDP binding, the loop spanning residues 291−302 being very important for this function. This also raises the possibility that there may be a substrate activation pathway via this flexible loop, in addition to the one uncovered in our studies.

SUPPORTING INFORMATION AVAILABLE

Kinetic curves at different pH values (Figures S1−S3) for WT and its W412F and W412A variants corresponding to the data listed in Tables 2−4. This material is available free of charge via the Internet at http://pubs.acs.org.

REFERENCES

1. Krampitz, L. O. (1969) *Annu. Rev. Biochem. 38*, 213−240.
2. Sable, H. Z., and Gubler, C. J., Eds. (1982) Thiamin: twenty years of progress, *Ann. N.Y. Acad. Sci. 378*, 7−122.
3. Kluger, R. (1987) *Chem. Rev. 87*, 863−876.
4. Schellenberger, A., and Schowen, R. L., Eds. (1988) *Thiamin Pyrophosphate Biochemistry*, Vol. 1−2, CRC Press, Boca Raton, FL.
5. Bisswanger, H., and Ullrich, J., Eds. (1991) *Biochemistry and Physiology of Thiamin Diphosphate Enzymes*, pp 1−453, VCH, Weinheim, Germany.
6. Bisswanger, H., and Schellenberger, A., Eds. (1996) *Biochemistry and Physiology of Thiamin Diphosphate Enzymes*, pp 1−599, A. u. C. Intemann, Wissenschaftlicher Verlag, Prien, Germany.
7. Jordan, F., Nemeria, N., Guo, F., Baburina, I., Gao, Y., Kahyaoglu, A., Li, H., Wang, J., Yi, J., Guest, J., and Furey, W. (1998) *Biochim. Biophys. Acta 1385*, 287−306.
8. Zeng, X., Farrenkopf, B., Hohmann, S., Dyda, F., Furey, W., and Jordan, F. (1993) *Biochemistry 32*, 2704−2709.
9. Baburina, I., Gao, Y., Hu, Z., Jordan, F., Hohmann, S., and Furey, W. (1994) *Biochemistry 33*, 5630−5635.
10. Baburina, I., Moore, D. J., Volkov, A., Kahyaoglu, A., Jordan, F., and Mendselsohn, R. (1996) *Biochemistry 35*, 10249−10255.
11. Baburina, I., Li, H., Bennion, B., Furey, W., and Jordan, F. (1998) *Biochemistry 37*, 1235−1244.
12. Baburina, I., Dikdan, G., Guo, F., Tous, G. I., Root, B., and Jordan, F. (1998) *Biochemistry 37*, 1245−1255.
13. Dyda, F., Furey, W., Swaminathan, S., Sax, M., Farrenkopf, B., and Jordan, F. (1993) *Biochemistry 32*, 6165−6170.
14. Arjunan, D., Umland, T., Dyda, F., Swaminathan, S., Furey, W., Sax, M., Farrenkopf, B., Gao, Y., Zhang, D., and Jordan, F. (1996) *J. Mol. Biol. 256*, 590−600.
15. Guo, F., Zhang, D., Kahyaoglu, A., Farid, R. S., and Jordan, F. (1998) *Biochemistry 37*, 13379−13391.
16. Jordan, F., Baburina, I., Gao, Y., Guo, F., Kahyaoglu, A., Nemeria, N., Volkov, A., Yi, J., Zhang, D., Machado, R., Guest, J., Furey, W., and Hohmann, S. (1996) in *Biochemistry and Physiology of Thiamin Diphosphate Enzymes* (Bisswanger, H., and Schellenberger, A., Eds.) pp 53−69, A. u. C. Intemann, Wissenschaftlicher Verlag, Prien, Germany.
17. Killenberg-Jabs, M., König, S., Eberhardt, I., Hohmann, S., and Hübner, G. (1997) *Biochemistry 36*, 1900−1905.
18. Kern, D., Kern, G., Neef, H., Tittmann, K., Killenberg-Jabs, M., Wikner, C., Schneider, G., and Hübner, G. (1997) *Science 275*, 67−70.
19. Wikner, C., Meshalkina, L., Nilsson, U., Nikkola, M., Lindqvist, Y., and Schneider, G. (1994) *J. Biol. Chem. 269*, 32144−32150.
20. Schenk, G., Leeper, F. J., England, R., Nixon, P. F., and Duggleby, R. G. (1997) *Eur. J. Biochem. 248*, 63−71.
21. Sarkar, G., and Sommer, S. S. (1990) *BioTechniques 8*, 404−407.
22. Li, H. (1999) Ph.D. Thesis, Rutgers University Graduate Faculty, Newark, NJ.
23. Ellis, K. J., and Morrison, J. F. (1982) *Methods Enzymol. 87*, 405−426.
24. Diefenbach, R. J., and Duggleby, R. G. (1991) *Biochem. J. 276*, 439−445.
25. Candy, M. J., and Duggleby, R. G. (1994) *Biochem. J. 300*, 7−13.
26. Furey, W., Arjunan, P., Chen, L., Sax, M., Guo, F., and Jordan, F. (1998) *Biochim. Biophys. Acta 1385*, 253−270.
27. Boiteux, A., and Hess, B. (1970) *FEBS Lett. 9*, 293−296.
28. Hübner, G., Weidhase, R., and Schellenberger, A. (1978) *Eur. J. Biochem. 92*, 175−181.
29. Lobell, M., and Crout, D. H. G. (1996) *J. Am. Chem. Soc. 118*, 1867−1873.
30. Alvarez, F. J., Ermer, J., Hübner, G., Schellenberger, A., and Schowen, R. L. (1995) *J. Am. Chem. Soc. 117*, 1678−1683.
31. Dietrich, A., and König, S. (1997) *FEBS Lett. 400*, 42−44.
32. Mücke, U., Wohlfahrt, T., Fiedler, U., Bäumlein, H., Rücknagel., K. P., and König, S. (1996) *Eur. J. Biochem. 237*, 373−382.
33. Lu, G., Dobritzsch, D., König, S., and Schneider, G. (1997) *FEBS Lett. 403*, 249−253.
34. Furey, W., Arjunan, P., Chen, L., Dyda, F., Umland, T., Swaminathan, S., Sax, M., Jordan, F., Farrenkopf, B., Gao, Y., and Zhang, D. (1996) in *Biochemistry and Physiology of Thiamin Diphosphate Enzymes* (Bisswanger, H., and Schellenberger, A., Eds.) pp 103−124, A. u. C. Intemann, Wissenschaftlicher Verlag, Prien, Germany.
35. Dobritzsch, D., König, S., Schneider, G., and Lu, G. (1998) *J. Biol. Chem. 273*, 20196−20204.
36. Eberhardt, I., Cederberg, H., Li, H., Konig, S., Jordan, F., and Hohmann, S. (1999) *Eur. J. Biochem. 262*, 191−201.

BI9902440